TECHNISCHE MECHANIK
an open access journal

journal homepage: www.ovgu.de/techmech

Tech. Mech., Vol. 45, Is. 1, (2025), 126–136

Received: 12.08.2025
Accepted: 10.11.2025
Available online: 10.11.2025

Computational Analysis of Non-Newtonian Blood Flow in a Human Arterial Bifurcation Model

Khellaf Belkhiri[1,2]*

[1] Mechanical Engineering Department, Faculty of Technology, University of M'Sila, 28000, M'Sila, Algeria
[2] Laboratory of Materials and Mechanics of Structures, University of M'Sila, 28000, M'Sila, Algeria

Abstract: Hemodynamic forces critically influence the pathogenesis of atherosclerotic lesions, particularly at anatomical sites characterized by intricate vascular geometries, such as arterial bifurcations. This study utilizes computational fluid dynamics (CFD) to investigate blood flow characteristics within a simplified three-dimensional model of the human aortic bifurcation, with particular attention to the transition of flow toward the carotid artery. Blood is modeled as an incompressible, non-Newtonian fluid using the Carreau–Yasuda model to capture shear-thinning behavior under physiological conditions. The simulations solve the incompressible Navier–Stokes equations using a finite volume method under steady-state conditions. Key hemodynamic parameters—including velocity fields, static pressure distributions, and wall shear stress (WSS) contours—are computed to assess flow disturbances and potential sites of vascular pathology. The results indicate complex flow features such as flow separation, recirculation zones, and stagnation points near the bifurcation apex. These regions correspond to areas of low and oscillatory WSS, which are clinically associated with endothelial dysfunction and the formation of atherosclerotic plaques. The findings demonstrate the effectiveness of CFD as a non-invasive diagnostic tool capable of elucidating local hemodynamic behavior and aiding in the assessment and treatment planning of vascular diseases, particularly those affecting cerebral perfusion.

Keywords: Arterial Bifurcation, Atherosclerosis, Non-Newtonian Blood Flow, Numerical Investigation, Wall Shear Stress, Computational Fluid Dynamics.

1 Introduction

The cardiovascular system is a complex network responsible for the transport of blood throughout the body. Although commonly modeled as a central pump connected to a series of vessels with varying resistance, this simplification overlooks the intricate interactions that define vascular physiology. The relationship between cardiac output and vascular resistance governs mean arterial pressure, which in turn regulates blood distribution across the system Fox and Rompolski (2021); Nichols et al. (2022).

Beyond its mechanical function, the vascular system operates as a dynamic organ, with the endothelium playing a vital role in regulating blood flow and interacting with circulating erythrocytes Caro (2012). Atherosclerosis, the most prevalent form of arteriosclerosis, remains a leading cause of mortality worldwide, contributing to nearly 31% of deaths in developed regions through its role in heart disease and stroke Furst (2019); Kassab (2019). Characterized by the formation of plaques that protrude into the arterial lumen, atherosclerosis restricts blood flow and creates thrombogenic surfaces, potentially leading to complete vessel occlusion.

Hemodynamic forces, particularly wall shear stress (WSS), are key contributors to the initiation and progression of atherosclerotic lesions. Regions of disturbed flow—such as arterial bifurcations and high-curvature segments—are frequently associated with abnormal shear patterns, including low and oscillatory WSS, which have been identified as predictors of plaque development Li et al. (2007); Zhang et al. (2012); Caro and Jaffrin (1995); Ku et al. (1985). The disease exhibits strong correlations with arterial geometry, wall mechanics, and the morphology of endothelial cells, all of which influence the local flow field and shear environment Lantz et al. (2011).

The interaction between blood flow and vessel walls generates pressure waves and induces mechanical deformation of the arterial structure. These coupled fluid-structure interactions further complicate the prediction of localized hemodynamic conditions Pakravan et al. (2015). Wall shear stress, in particular, is highly sensitive to near-wall velocity gradients and can be significantly affected by arterial wall compliance Sarraju and Nissen (2024).

Advances in computational resources and numerical methods have positioned computational fluid dynamics (CFD) as a powerful tool in cardiovascular research. CFD enables detailed investigation of complex flow phenomena within realistic vascular geometries, allowing for non-invasive analysis of clinically relevant parameters Kiris et al. (1997); Lei et al. (1997); Hyun et al. (2000); Leuprecht and Perktold (2001). In particular, arterial bifurcations represent critical regions of interest due to their propensity for disturbed flow, thrombus formation, and plaque accumulation Belkhiri and Boumeddane (2021).

The most critical hemodynamic complications are widely recognized to arise from the complex flow structures within arterial bifurcations. Key challenges stemming from fluid dynamic phenomena in these regions include the following: (i) Flow separation and secondary recirculation zones contribute to prolonged residence time of blood near the vessel wall, promoting thrombogenesis

* E-mail address: khellaf.belkhiri@univ-msila.dz
doi: 10.24352/UB.OVGU-2025-045

and increasing the risk of clot formation;(ii) Elevated turbulent shear stresses may lead to mechanical damage of erythrocytes and activation of platelets, both of which are implicated in pathological processes such as hemolysis and thrombus development; and (iii) Significant pressure losses across bifurcated segments increase the workload on the heart, thereby compromising circulatory efficiency and potentially contributing to long-term cardiovascular dysfunction.
The present study investigates steady, laminar blood flow through a simplified three-dimensional model of a human arterial bifurcation. Emphasis is placed on analyzing velocity fields and wall shear stress distributions under physiological flow conditions, incorporating the non-Newtonian behavior of blood. The objective is to enhance understanding of the local hemodynamic environment associated with atherogenesis and thromboembolic risk in bifurcated arterial segments.

2 Methods

Accurate simulation of blood flow through a human arterial bifurcation necessitates the incorporation of physiologically realistic conditions. Essential modeling requirements include anatomically representative bifurcation geometry, appropriate physiological flow rates, the rheological characterization of blood as a non-Newtonian fluid, and consideration of the mechanical behavior of the vessel wall. In the present computational approach, these factors were addressed to the extent appropriate for an initial investigation.

2.1 Geometric Model

A simplified three-dimensional arterial bifurcation geometry was constructed to represent a generic human arterial junction, as illustrated in Fig. 1. The model was developed to capture key geometric features relevant to bifurcation hemodynamics while allowing for computational tractability. In this preliminary study, The flow rate ratio between the branches is set to 70:30 % and the arterial walls were assumed to be rigid and non-deformable to isolate the effects of flow dynamics.

2.2 Fluid Properties

Blood was modeled as an incompressible, non-Newtonian fluid with a constant density of 1056 kg/m^3 and a reference dynamic viscosity of 0.0034 Pa · s, consistent with established rheological data Perktold and Peter (1990). The non-Newtonian behavior was incorporated using an appropriate viscosity model to account for shear-thinning effects characteristic of blood under physiological conditions.

2.3 Constitutive Model

Blood exhibits complex non-Newtonian behavior, characterized by shear-dependent viscosity and viscoelastic properties that vary with both shear rate and time Thurston (1979). The primary factors influencing blood rheology include plasma viscosity, red blood cell (RBC) aggregation, and the deformability of RBCs. However, in large and medium-sized arteries, the particulate nature of blood can be neglected, allowing it to be modeled as a homogeneous, incompressible, non-Newtonian, and inelastic fluid. Under physiological shear rates typical of these vessels, blood demonstrates shear-thinning behavior, where apparent viscosity decreases with increasing shear rate. This behavior can be effectively captured using empirical viscosity models designed for non-Newtonian fluids, enabling accurate representation of blood flow dynamics in arterial simulations Perktold and Rappitsch (1995); Belkhiri and Boumeddane (2021).
Red blood cells (RBCs) comprise the majority of the cellular volume in blood, making hematocrit (Ht)—the volume fraction of RBCs—a primary determinant of blood viscosity Chien (1987). In contrast, white blood cells (WBCs) and platelets exist at much

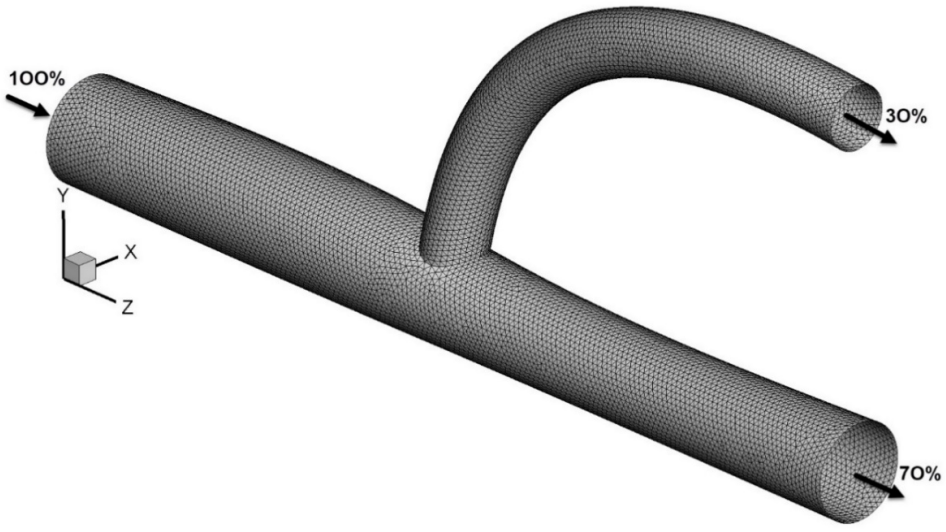

Fig. 1: Geometry of the arterial bifurcation

lower concentrations and have negligible influence on the rheological behavior of blood in large vessels. At low shear rates, RBCs tend to aggregate into rouleaux formations, resulting in elevated apparent viscosity. As shear rate increases, these aggregates disassociate, leading to a reduction in viscosity (Fig. 2). This shear-dependent aggregation-disaggregation behavior contributes to the non-Newtonian characteristics of blood flow.
In microcirculation (e.g., capillaries), the discrete nature of RBCs and their deformability significantly influence flow dynamics, requiring particle-resolved or microscale modeling approaches Chien (1987). However, in large arteries, where blood can be treated as a continuum, the shear-thinning behavior of blood can be effectively modeled using the Carreau–Yasuda constitutive equation Gijsen et al. (1999); Ramezanpour et al. (2019); Santesarti et al. (2025). Under these conditions, the relationship between shear rate and apparent viscosity is expressed as:

$$\boldsymbol{\tau} = 2\mu(\dot{\gamma})\mathbf{D} \tag{1}$$

where $\boldsymbol{\tau}$ is the shear stress tensor, $\mu(\dot{\gamma})$ is the shear rate-dependent dynamic viscosity, $\dot{\gamma}$ is the shear rate (rate of shear strain), and $\mathbf{D}$ is the strain rate tensor, defined as:

$$\mathbf{D} = \frac{1}{2}\left(\nabla\mathbf{V} + \nabla\mathbf{V}^{\top}\right) \tag{2}$$

where $\mathbf{V}$ is the velocity vector.

The occurring shear rate $\dot{\gamma}$ is obtained from the second invariant D_{II} of the strain rate tensor such that:

$$\dot{\gamma} = 2\sqrt{D_{II}} \tag{3}$$

The generalized Carreau-Yasuda model is as follows:

$$\boldsymbol{\tau} = 2\left[\mu_{\infty} + \frac{\mu_0 - \mu_{\infty}}{\left[1 + (\lambda\,|\dot{\gamma}|)^a\right]^{\frac{(1-n)}{a}}}\right]\mathbf{D} \tag{4}$$

where λ, a, and n are model parameters, with μ_0 and μ_{∞} being the viscosities at zero and infinite shear rates, respectively. This formulation provides an accurate representation of blood viscosity across the physiological shear rate range.

2.4 Governing Equations

Under the assumptions of steady, incompressible, laminar flow, the governing equations for blood flow in the arterial bifurcation are described by the three-dimensional continuity and Navier–Stokes equations Kleinstreuer (1997):

$$\nabla \cdot \mathbf{V} = 0 \tag{5}$$

$$\rho(\mathbf{V} \cdot \nabla\mathbf{V}) = -\nabla p + \nabla \cdot \boldsymbol{\tau} \tag{6}$$

where $\mathbf{V}$ is the velocity vector, p is the pressure, and $\boldsymbol{\tau}$ is the shear stress tensor.

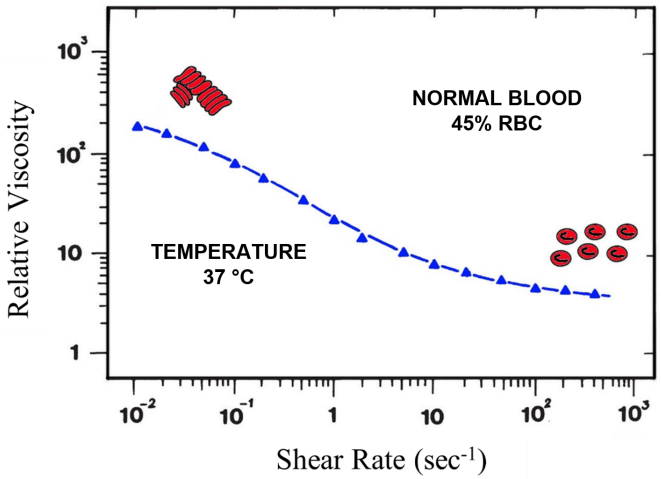

Fig. 2: Apparent viscosity μ_a, as a function of the shear rate $\dot{\gamma}$ (adapted from Chien (1987))

The complex rheological behavior of blood is approximated using a shear-thinning model, where the apparent viscosity is expressed as a function of the shear rate. From Eq. (4), an explicit relation for the effective non-Newtonian viscosity $\mu = \mu(D_{II})$ Ramezanpour et al. (2019) is derived as:

$$\mu = \mu_\infty + (\mu_0 - \mu_\infty)\,[1 + (\lambda|\dot{\gamma}|)^a]^{\frac{n-1}{a}} \tag{7}$$

The advantage of the Carreau–Yasuda model over other models is the additional shear-rate modifier, λ, which allows for a better fit to blood rheological data in the low shear rate range (i.e., $\dot{\gamma} \sim 10^{-2}$ s^{-1}). The coefficients used in the Carreau–Yasuda model for a normal hematocrit level of 45% were taken as: $\mu_\infty = 2.2 \times 10^{-3}$ Pa · s, $\mu_0 = 22 \times 10^{-3}$ Pa · s, $\lambda = 0.11$ s, $a = 0.644$, and $n = 0.392$ Gijsen et al. (1999); Kabinejadian and Ghista (2012); Sherwood et al. (2014); Ramezanpour et al. (2019). The local shear rate, $\dot{\gamma}$, used in the viscosity equation is computed from the second scalar invariant of the rate of deformation tensor.

2.5 Boundary Conditions

For three-dimensional incompressible flow, Eqs. (5) and (6) represent a system of four coupled partial differential equations: three momentum equations corresponding to the velocity components and one continuity equation enforcing mass conservation. This system is well-posed and numerically solvable when supplemented with suitable boundary conditions.
The specification of appropriate boundary conditions is critical to accurately resolving the flow field. In the present study, the applied boundary conditions are as follows:

- Inlet: A fully developed, steady, laminar velocity profile is imposed at the inlet plane. The mean inlet velocity U_{in} is prescribed based on physiological flow rates (typically 0.1–0.35 m/s). The three-dimensional inlet velocity field is given by:

$$\mathbf{V}(r) = \left[2U_{\text{in}}\left(1 - \left(\frac{r}{R}\right)^2\right)\right]\mathbf{e}_z \tag{8}$$

where $r = \sqrt{x^2 + y^2}$ is the radial coordinate from the vessel centerline, R is the inlet radius, and $\mathbf{e}_z$ is the unit vector in the axial direction.

- Outlets: The stress-free outflow boundary condition is applied at all the outlets of the artery bifurcation Perktold et al. (1991); Van der Giessen et al. (2011). This can be described mathematically by the condition:

$$(-p\mathbf{I} + \boldsymbol{\tau}) \cdot \mathbf{n} = \mathbf{0} \tag{9}$$

where $\mathbf{I}$ is the identity tensor, and $\mathbf{n}$ is the outward pointing unit vector at the outflow boundary.

- Walls: The arterial walls are assumed rigid with a no-slip velocity condition ($\mathbf{v} = \mathbf{0}$). No wall motion or compliance is considered in this study.

2.6 Computational Fluid Dynamics Setup

The computational domain represents an arterial bifurcation consisting of a primary vessel (trunk) and a daughter branch, as illustrated in Fig. 1. The domain was discretized using the finite volume method, subdividing the geometry into a large number of control volumes for numerical solution of the governing equations.
Mesh generation is a critical step in CFD modeling, particularly for complex vascular geometries. In this study, the domain was discretized into control volumes using an unstructured grid composed primarily of tetrahedral elements, which offer flexibility for capturing the complex geometry of the bifurcation. To resolve the near-wall gradients with sufficient accuracy, six inflation (prism) layers were applied adjacent to all wall boundaries, enhancing the resolution of wall shear stress and boundary layer development. To improve mesh quality and ensure stable numerical performance, straight cylindrical extensions were added to both the inlet and outlet of the bifurcation model. These extensions allow the flow to develop fully before entering the region of interest and to exit smoothly, thereby minimizing boundary effects and reducing computational cost. These regions were meshed with structured hexahedral elements, allowing for efficient and accurate resolution of fully developed inflow and outflow conditions.
All transport equations were discretized using second-order accurate spatial schemes. A high-resolution upwind scheme was employed to minimize numerical diffusion, particularly in regions of strong velocity gradients. Whenever possible, a second-order upwind Euler scheme was applied; in cases where solution boundedness was at risk, the solver reverted to a first-order upwind scheme. These flux computations were based on control-volume integration techniques, as described by Patankar Patankar (1980) and Blazek Blazek (2015).
Numerical simulations were performed using the finite volume solver, ANSYS Fluent, which solves the transport equations, including the Navier-Stokes equations. A high-resolution scheme for advection was implemented to mitigate numerical diffusion. A second-order upwind Euler scheme was employed where feasible, transitioning to a first-order upwind Euler scheme when a bounded solution was required. The iterative solution procedure for the discrete equations is based on the SIMPLE method, with a preconditioned conjugate gradient algorithm used to calculate pressure corrections. The governing equations are integrated over each control volume using the finite volume method, resulting in a discrete system of algebraic equations expressed as:

$$A_P\,\phi_P - \sum_{\text{nb}} A_{\text{nb}}\,\phi_{\text{nb}} = S_u \tag{10}$$

where ϕ denotes the dependent variable (e.g., velocity components), S_u represents the source term, and the subscript "nb" refers to the neighboring nodes of the control volume. The coefficients A_P and A_{nb} correspond to the central node and its neighbors, respectively. The diagonal coefficient A_P is determined by the contributions of diffusion and convection fluxes, ensuring numerical stability and accuracy. The diagonal coefficient of the matrix, A_P, is defined as:

$$A_P = \sum_{\text{nb}} A_{\text{nb}} - S_P + C_U - C_D + C_N - C_S + C_E + C_W \tag{11}$$

where C_U, C_D, C_N, C_S, C_E, and C_W are the convection flux coefficients at the respective control volume faces, identified by their directional subscripts (up, down, north, south, east, and west). The summation of these convection coefficients represents the net convective transport across the control volume boundaries. In a fully converged solution, this sum satisfies mass conservation and thus approaches zero.
To assess numerical convergence, the residual root mean square (RMS) method was employed. The convergence criterion was defined by a residual threshold of 10^{-5} for both the momentum and continuity equations in all simulations conducted in this study.

3 Numerical Results and Discussion

The results presented in this section provide a comprehensive analysis of the flow characteristics within the arterial bifurcation model. Particular attention is given to the velocity field, the formation and extent of recirculation zones, and the distribution of wall shear stress (WSS) along the arterial walls. Of special interest is the identification and characterization of regions that exhibit flow reversal, which are critical to understanding the hemodynamic factors associated with atherogenesis. All computations were performed under steady-state flow conditions, allowing for detailed evaluation of the spatial patterns of velocity and WSS throughout the bifurcated geometry.

3.1 Model Validation

To assess the accuracy and applicability of the present CFD simulations, a validation was performed against the well-known experimental and numerical results reported by Gijsen et al. (1999) Gijsen et al. (1999). In their study, they investigated steady, laminar flow in an idealized carotid bifurcation geometry using both Laser Doppler Anemometry (LDA) measurements and finite-element simulations, incorporating a non-Newtonian Carreau-Yasuda model to describe the shear-thinning behavior of blood. Their results have been widely adopted as a benchmark for validating hemodynamic simulations in large arteries. Fig. 3 illustrates the comparison of the axial velocity profile obtained in the arterial bifurcation at a downstream location of $Z = 2D$, where D is the inlet diameter. The velocity distribution predicted by the current CFD model closely follows the experimental and numerical profiles reported by Gijsen et al. (1999) Gijsen et al. (1999), capturing the same peak velocity location and profile asymmetry near the outer wall of the bifurcation. This good qualitative agreement demonstrates that the present computational approach reliably predicts the main hemodynamic features within the bifurcation region.

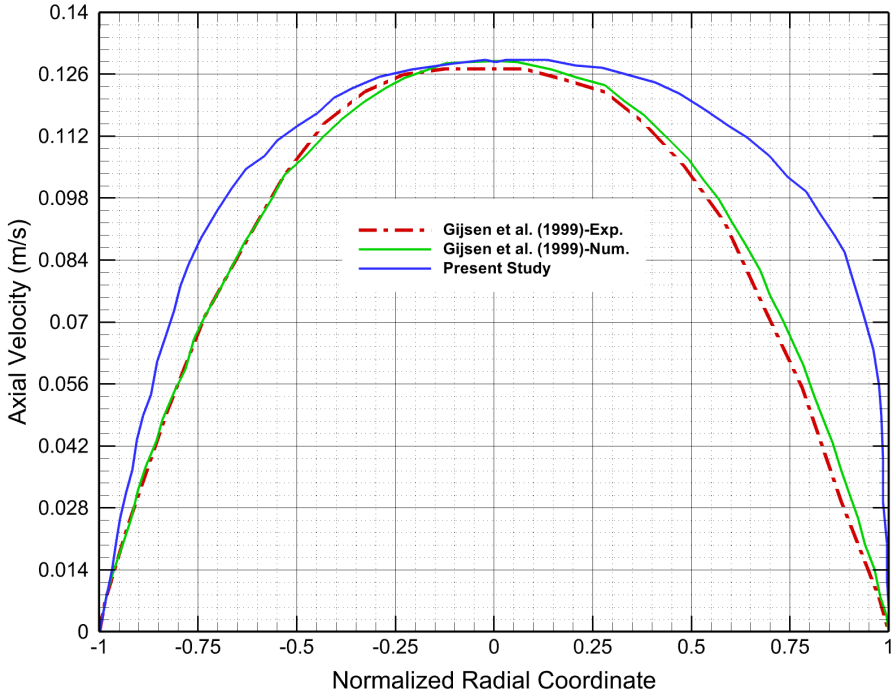

Fig. 3: Comparison of axial velocity profiles between the present CFD simulation and the experimental/numerical results of Gijsen et al. (1999)

3.2 Flow Fields

Streamlines, which effectively illustrate the fundamental characteristics of blood flow within arterial bifurcations, offer critical insights into complex flow patterns. Fig. 4 presents the computed streamlines colored by the magnitude of the axial velocity, effectively capturing the primary features of blood flow within the bifurcation region. Notably, the figure clearly reveals zones of flow separation, recirculation, and stagnation in the vicinity of the bifurcation junction.

These recirculation zones are of particular physiological significance, as they are known to increase near-wall residence time, promote platelet activation, and facilitate the formation of fibrin thrombi—factors that contribute to the development of intimal hyperplasia and thrombosis Kabinejadian and Ghista (2012). The stagnated flow patterns observed in the simulation suggest a high likelihood of thrombus formation due to platelet accumulation in these low-shear regions, consistent with prior experimental and computational findings Ku et al. (1985); Karner et al. (1999).

An important parameter of interest in hemodynamic analysis is the velocity vector field, which captures the directional behavior and magnitude of flow throughout the fluid domain. In arterial bifurcations, this field is significantly influenced by the jet-like inflow generated by ventricular contraction, producing complex flow structures downstream of the junction.

Figures 5 and 6 present the velocity contours in the longitudinal symmetry plane and in transverse cross-sections orthogonal to the bifurcation plane, respectively. The results demonstrate that flow directed toward the inferior wall of the parent (common) artery induces vortex structures in the vicinity of the bifurcation apex. A prominent flow separation region is observed along the superior wall of the daughter vessel, indicative of disturbed flow conditions. These regions of low velocity and reversed flow are hemodynamically unfavorable and are commonly associated with increased risk for thrombus formation and atherogenesis. Specifically, flow stagnation and recirculation at the upper region of the bifurcation and the inferior wall of the branch vessel suggest susceptibility to platelet aggregation and clot formation.

Of particular note is the identification of a stagnation zone within the daughter branch, a site frequently implicated in the early development of atherosclerotic lesions Perktold et al. (1994). These flow disturbances correlate with regions of low and oscillatory wall shear stress—recognized factors in the pathogenesis of intimal thickening and vascular remodeling.

Fig. 7 illustrates axial velocity profiles at various cross-sections within the branching plane. Upstream of the bifurcation, the velocity distribution in the parent artery remains symmetric and stable. However, in the daughter branches, highly asymmetric profiles emerge, particularly under elevated flow rates. These profiles exhibit peak velocities skewed toward the inner (divider) walls, while the velocity diminishes near the outer walls. This asymmetry results in elevated wall shear stress on the flow divider side and reduced shear on the outer walls, contributing to spatial variations in hemodynamic forces. The degree of skewness is observed to intensify along the axial flow direction, reflecting the influence of geometry-induced secondary flows.

Fig. 8 presents a three-dimensional visualization of the axial velocity vectors within the bifurcation, mapped across multiple cross-sectional planes along the flow direction. This representation captures the spatial evolution of the velocity field and highlights regions of recirculating flow near the branching zone. Notably, a more intricate and disturbed flow pattern is observed near the flow divider region (at $Z = 25$ mm), characterized by pronounced changes in flow direction and magnitude. The results reveal distinct zones of flow separation and vortex formation within the daughter branch, indicative of complex hemodynamic behavior typically associated with bifurcated geometries.

In Fig. 9, the velocity vector field is depicted within the branching plane of the arterial bifurcation. The flow pattern reveals extended vortical structures in the vicinity of the bifurcation zone and notably reduced velocities near the outer (non-dividing) wall

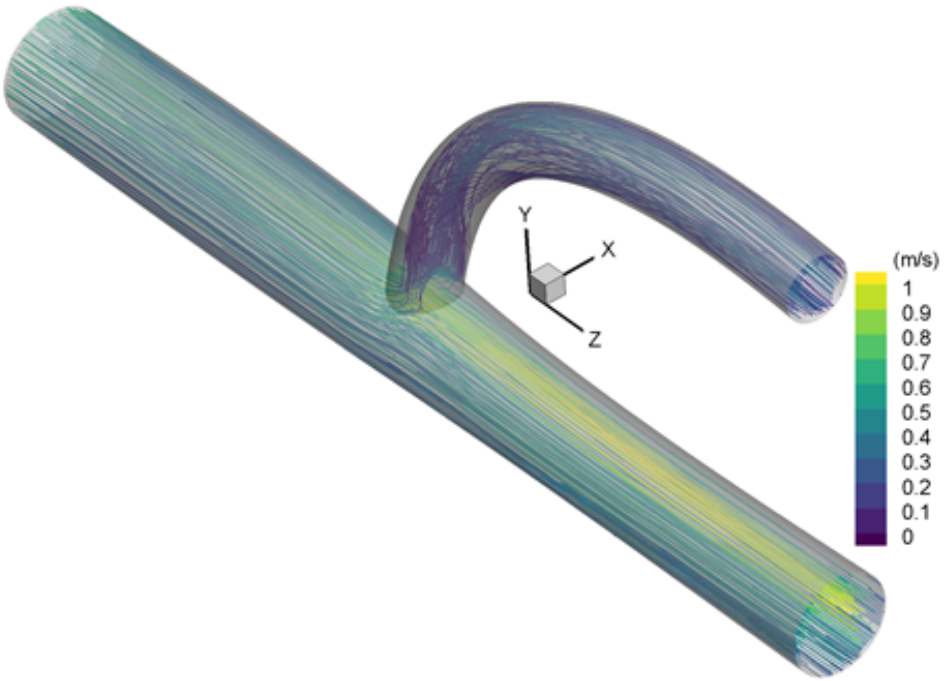

Fig. 4: Computed streamlines contours

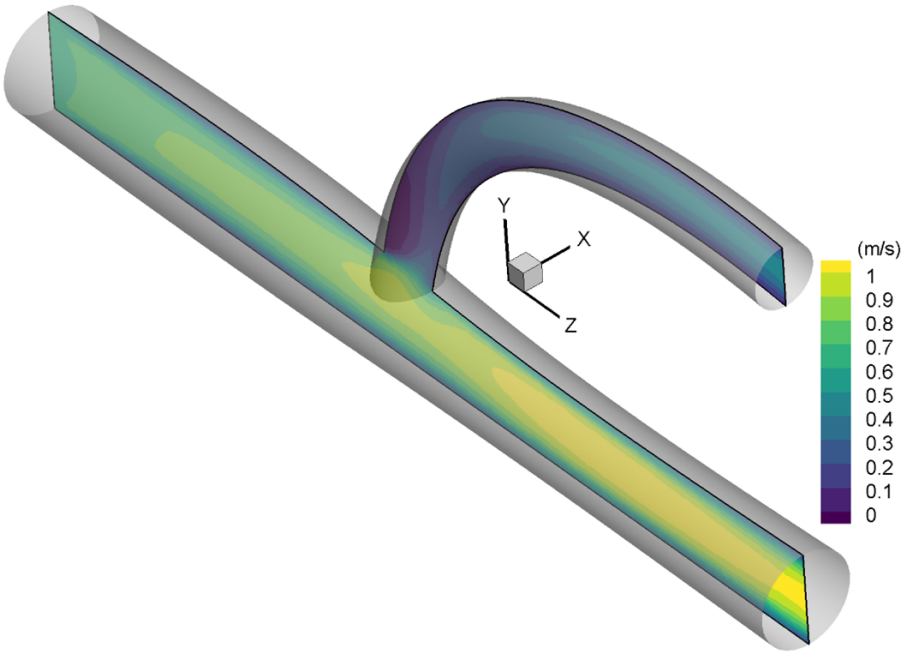

Fig. 5: Axial velocity magnitude contours in the branching plane

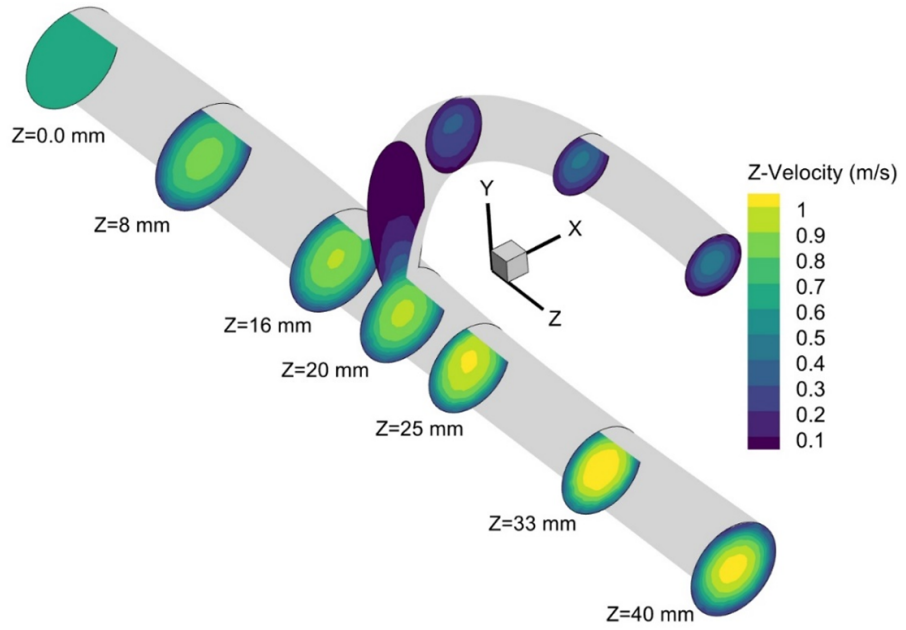

Fig. 6: Axial velocity magnitude contours along sections perpendicular to the bifurcation plane

of the daughter branch. Two distinct regions of flow reversal are observed: a primary recirculation zone within the daughter branch and a smaller secondary reverse flow region located near the outer corner of the common arterial junction. These features highlight the complex flow environment induced by the geometric bifurcation, characterized by separation, eddy formation, and reversed flow. Such hemodynamic disturbances are of particular interest, as they are strongly correlated with pathophysiological processes including thrombogenesis, intimal hyperplasia, and the progression of atherosclerotic lesions.

3.3 Wall Shear Stress

In the cardiovascular system, wall shear stress (WSS) plays a pivotal role in vascular health and disease. Excessively high WSS values can result in direct endothelial cell injury, whereas abnormally low WSS is associated with increased risks of atherogenic processes such as arteriosclerotic plaque deposition, hemolysis, and thrombus formation Malek et al. (1999). Furthermore, WSS is instrumental in elucidating the mechanisms underlying both the progression and potential regression of atherosclerotic stenosis Archie (1998).

Wall shear stress (WSS) is widely regarded as a key hemodynamic factor influencing endothelial cell function along arterial walls. While low WSS is commonly implicated in the initiation and development of atherosclerotic lesions, recent studies have also identified pathological responses under high shear stress conditions Cecchi et al. (2011); De Wilde et al. (2016).

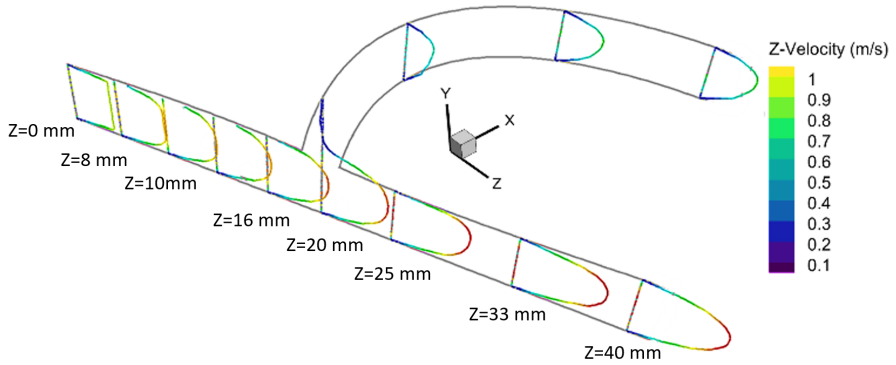

Fig. 7: Axial velocity profiles in the bifurcation plane

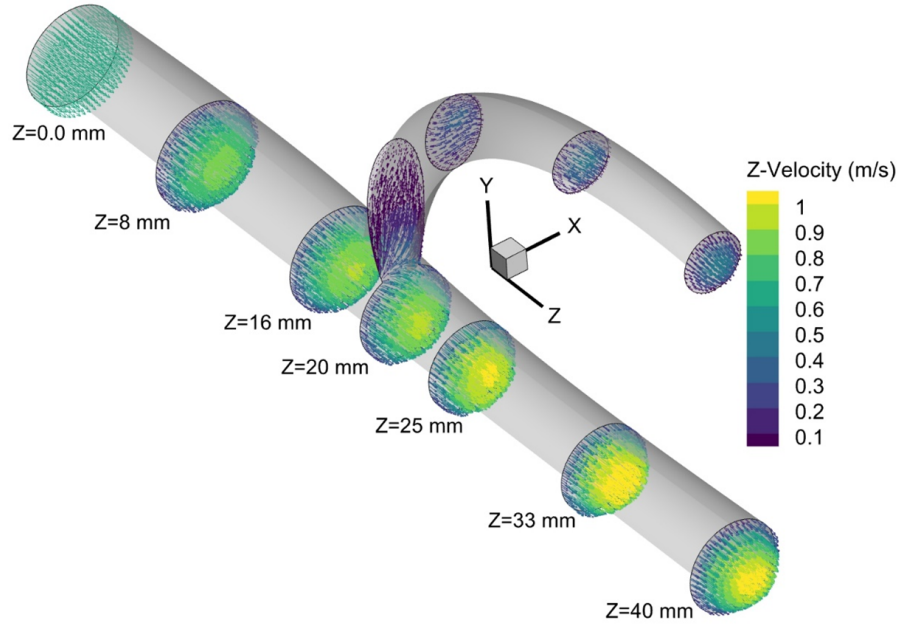

Fig. 8: Axial velocity vector field along sections perpendicular to the bifurcation plane

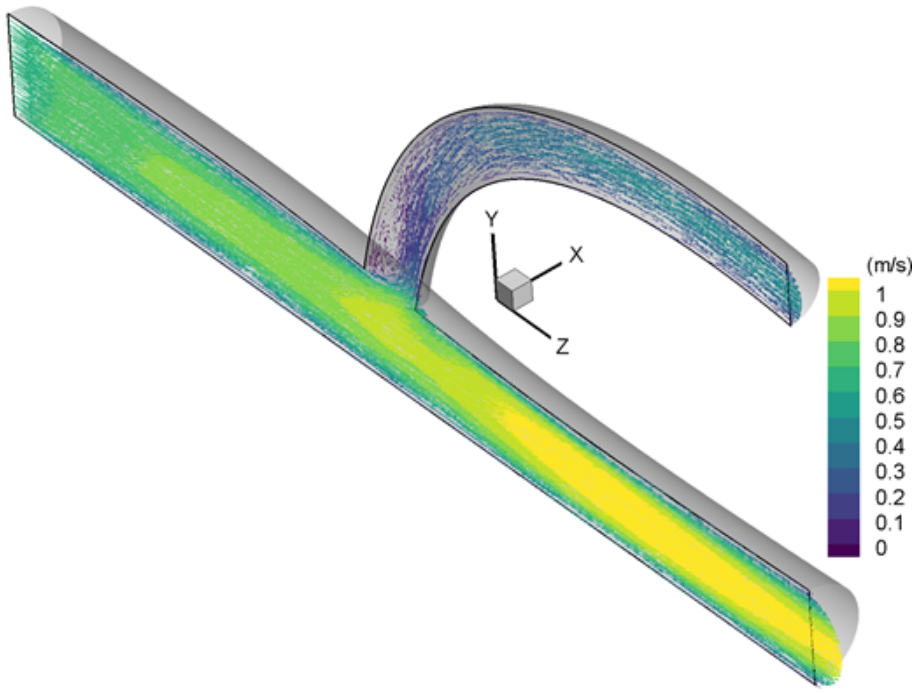

Fig. 9: Axial velocity vector field in the branching plane of the model

Fig. 10 illustrates the computed WSS distribution along the arterial bifurcation. Elevated WSS values are observed at the branch entrance near the flow divider and upstream of the bifurcation in the main artery. In contrast, low-WSS regions are evident along the outer walls of the bifurcation, which are prone to plaque formation due to reduced shear-mediated endothelial shear-mediated endothelial stimulation.

These computational results are consistent with clinical evidence indicating that persistent low-WSS regions are highly susceptible to atherosclerotic plaque development. Moreover, the presence of such plaques and associated geometric irregularities leads to localized stress concentrations. This phenomenon is of clinical importance, as stress accumulation within plaques increases the likelihood of rupture, potentially resulting in thrombotic occlusion or distal embolization.

4 Conclusions

This study demonstrates the utility of computational fluid dynamics (CFD) in analyzing the complex hemodynamic environment within arterial bifurcations. The numerical simulations provide detailed insights into velocity fields, recirculation zones, and wall shear stress (WSS) distributions, all of which are critical in understanding vascular pathologies such as atherosclerosis and thrombosis.

CFD has emerged as a valuable tool in cardiovascular research, enabling the noninvasive prediction of blood flow behavior and associated biomechanical forces that are otherwise difficult to measure experimentally. In particular, it offers a powerful means for identifying regions of abnormal WSS, which are strongly correlated with endothelial dysfunction and the initiation of plaque formation. The present analysis, conducted using a finite volume-based solver (ANSYS Fluent), solves the incompressible Navier–Stokes equations for non-Newtonian blood rheology modeled via the Carreau–Yasuda formulation.

The results confirm that blood flow in arterial bifurcations is characterized by complex secondary flows, flow separation, and recirculation regions. These features contribute to spatially heterogeneous WSS distributions. Regions of low WSS, identified in the outer walls of the bifurcation and along stagnation zones, are especially susceptible to atherogenesis due to prolonged residence times and reduced endothelial shear stimulation. Conversely, high WSS values near the flow divider correspond to steep velocity gradients, indicative of high shear-induced stresses on the arterial wall.

While the model captures key hemodynamic characteristics, certain simplifications must be acknowledged. The simulations assume steady-state flow and rigid, non-compliant arterial walls, which deviate from physiological conditions where pulsatile flow and wall elasticity significantly influence flow dynamics. Future investigations should incorporate pulsatile boundary conditions and fluid–structure interaction (FSI) models to account for arterial wall distensibility, thereby enhancing the physiological fidelity of the simulations.

Despite these limitations, the study demonstrates that CFD modeling can effectively characterize flow phenomena of clinical relevance and provides a foundation for more sophisticated patient-specific analyses. Such computational frameworks may support diagnostic and therapeutic planning in vascular medicine, particularly for cerebrovascular diseases involving compromised blood supply to the brain.

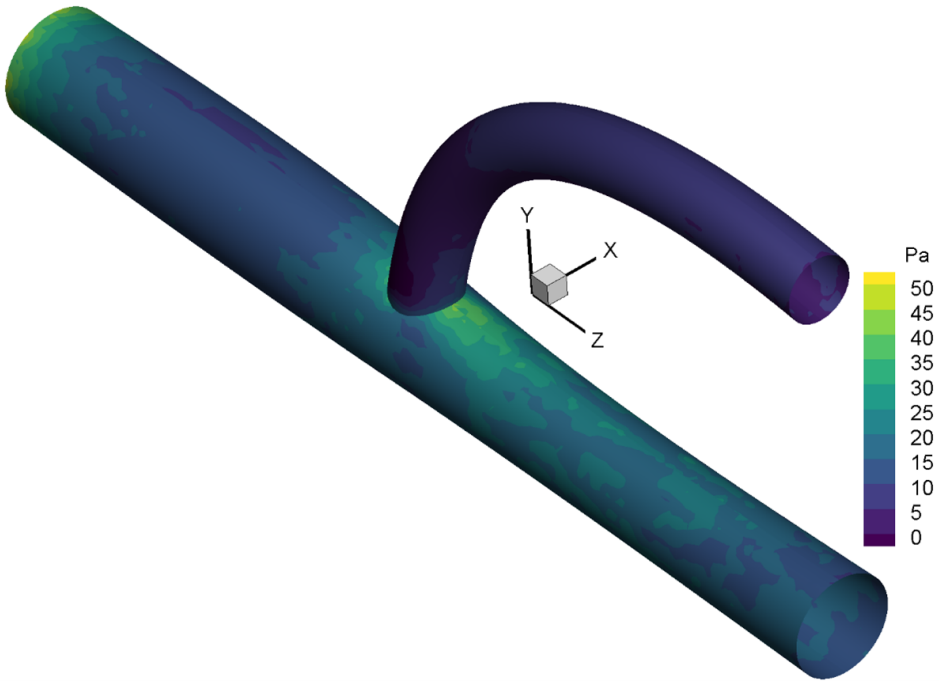

Fig. 10: Wall shear stress (WSS) contours

Acknowledgment

The author would like to thank Professor Karl Perktold for his help. The author affirms that artificial intelligence tools were used exclusively for language editing and stylistic refinement in the preparation of this manuscript. All research concepts, methodological frameworks, data analyses, interpretations, and conclusions are entirely the result of the author's original work and intellectual contribution.

References

J. P. Archie. The outcome of external carotid endarterectomy during routine carotid endarterectomy. *Journal of Vascular Surgery*, 28(4):585–90, 1998. doi: 10.1016/s0741-5214(98)70080-1.

K. Belkhiri and B. Boumeddane. A Cartesian grid generation technique for 2-D non-Newtonian blood flow through a bileaflet mechanical heart valve. *International Journal for Computational Methods in Engineering Science and Mechanics*, 22(4): 297–315, 2021. doi: 10.1080/15502287.2021.1871677.

J. Blazek. *Computational Fluid Dynamics : Principles and Applications*. Butterworth-Heinemann, New York, 3rd edition, 2015.

C. G. Caro. *The Mechanics of the Circulation*. Cambridge University Press, 2nd edition, 2012. doi: 10.1017/CBO9781139013406.

C. G. Caro and M. Y. Jaffrin. *Biological Flows*. Springer US, New York, NY, 1995. doi: 10.1007/978-1-4757-9471-7.

E. Cecchi, C. Giglioli, S. Valente, C. Lazzeri, G. F. Gensini, R. Abbate, and L. Mannini. Role of hemodynamic shear stress in cardiovascular disease. *Atherosclerosis*, 214(2):249–56, 2011. doi: 10.1016/j.atherosclerosis.2010.09.008.

S. Chien. Clinical hemorheology: Applications in cardiovascular and hematological disease, diabetes, surgery and gynecology. In S. Chien, J. Dormandy, E. Ernst, and A. Matrai, editors, *Physiological and Pathophysiological Significance of Hemorheology*, pages 125–164. Springer Netherlands, 1987. doi: 10.1007/978-94-009-4285-1_5.

D. De Wilde, B. Trachet, N. Debusschere, F. Iannaccone, A. Swillens, J. Degroote, J. Vierendeels, G. R. Y. De Meyer, and P. Segers. Assessment of shear stress related parameters in the carotid bifurcation using mouse-specific FSI simulations. *Journal of Biomechanics*, 49(11):2135–2142, 2016. doi: 10.1016/j.jbiomech.2015.11.048.

S. I. Fox and K. Rompolski. *Human Physiology*. McGraw-Hill Education, New York, NY, 16th edition, 2021.

B. Furst. *The Heart and Circulation: An Integrative Model*. Springer International Publishing, Switzerland AG, 2019. doi: 10.1007/978-3-030-25062-1.

F. J. Gijsen, F. N. van de Vosse, and J. D. Janssen. The influence of the non-Newtonian properties of blood on the flow in large arteries: steady flow in a carotid bifurcation model. *Journal of Biomechanics*, 32(6):601–608, 1999. doi: 10.1016/s0021-9290(99)00015-9.

S. Hyun, C. Kleinstreuer, and J. P. Archie. Hemodynamics analyses of arterial expansions with implications to thrombosis and restenosis. *Medical Engineering & Physics*, 22(1):13–27, 2000. doi: 10.1016/s1350-4533(00)00006-0.

F. Kabinejadian and D. N. Ghista. Compliant model of a coupled sequential coronary arterial bypass graft: effects of vessel wall elasticity and non-newtonian rheology on blood flow regime and hemodynamic parameters distribution. *Medical Engineering & Physics*, 34(7):860–872, 2012. doi: 10.1016/j.medengphy.2011.10.001.

G. Karner, K. Perktold, M. Hofer, and D. Liepsch. Flow characteristics in an anatomically realistic compliant carotid artery bifurcation model. *Computer Methods in Biomechanics and Biomedical Engineering*, 2(3):171–185, 1999. doi: 10.1080/10255849908907986.

G. S. Kassab. *Coronary Circulation: Anatomy, Mechanical Properties, and Biomechanics*. Springer International Publishing, Switzerland AG, 2019. doi: 10.1007/978-3-030-14819-5.

C. Kiris, D. Kwak, S. Rogers, and I. D. Chang. Computational approach for probing the flow through artificial heart devices. *Journal of Biomechanical Engineering*, 119(4):452–460, 1997. doi: 10.1115/1.2798293.

C. Kleinstreuer. *Engineering Fluid Dynamics: An Interdisciplinary Systems Approach*. Cambridge University Press, 1997. doi: 10.1017/CBO9781139174510.

D. N. Ku, D. P. Giddens, C. K. Zarins, and S. Glagov. Pulsatile flow and atherosclerosis in the human carotid bifurcation. positive correlation between plaque location and low oscillating shear stress. *Arteriosclerosis*, 5(3):293–302, 1985. doi: 10.1161/01.atv.5.3.293.

J. Lantz, J. Renner, and M. Karlsson. Wall shear stress in a subject specific human aorta—influence of fluid-structure interaction. *International Journal of Applied Mechanics*, 03(4):759–778, 2011. doi: 10.1142/S1758825111001226.

M. Lei, C. Kleinstreuer, and J. P. Archie. Hemodynamic simulations and computer-aided designs of graft-artery junctions. *Journal of Biomechanical Engineering*, 119(3):343–348, 1997. doi: 10.1115/1.2796099.

A. Leuprecht and K. Perktold. Computer simulation of non-Newtonian effects on blood flow in large arteries. *Computer Methods in Biomechanics and Biomedical Engineering*, 4(2):149–63, 2001. doi: 10.1080/10255840008908002.

M. X. Li, J. J. Beech-Brandt, L. R. John, P. R. Hoskins, and W. J. Easson. Numerical analysis of pulsatile blood flow and vessel wall mechanics in different degrees of stenoses. *Journal of Biomechanics*, 40(16):3715–3724, 2007. doi: 10.1016/j.jbiomech.2007.06.023.

A. M. Malek, S. L. Alper, and S. Izumo. Hemodynamic shear stress and its role in atherosclerosis. *Jama*, 282(21):2035–2042, 1999. doi: 10.1001/jama.282.21.2035.

W. W. Nichols, M. O'Rourke, E. R. Edelman, and C. Vlachopoulos. *McDonald's Blood Flow in Arteries: Theoretical, Experimental and Clinical Principles*. CRC Press, London, 2022. doi: 10.1201/b13568.

A. H. Pakravan, M. S. Saidi, and B. Firoozabadi. FSI simulation of a healthy coronary bifurcation for studying the mechanical stimuli of endothelial cells under different physiological conditions. *Journal of Mechanics in Medicine and Biology*, 15(5): 1550089, 2015. doi: 10.1142/s021951941550089x.

S. V. Patankar. *Numerical Heat Transfer and Fluid Flow*. Series in computational methods in mechanics and thermal sciences. Hemisphere Pub. Corp. ; McGraw-Hill, 1980.

K. Perktold and R. Peter. Numerical 3D-simulation of pulsatile wall shear stress in an arterial t-bifurcation model. *Journal of Biomedical Engineering*, 12(1):2–12, 1990. doi: 10.1016/0141-5425(90)90107-X.

K. Perktold and G. Rappitsch. Mathematical modeling of arterial blood flow and correlation to atherosclerosis. *Technology and Health Care*, 3:139–151, 1995. doi: 10.3233/THC-1995-3301.

K. Perktold, M. Resch, and H. Florian. Pulsatile non-Newtonian flow characteristics in a three-dimensional human carotid bifurcation model. *Journal of Biomechanical Engineering*, 113(4):464–475, 11 1991. doi: 10.1115/1.2895428.

K. Perktold, E. Thurner, and Th Kenner. Flow and stress characteristics in rigid walled and compliant carotid artery bifurcation models. *Medical & Biological Engineering & Computing*, 32(1):19–26, 1994. doi: 10.1007/BF02512474.

M. Ramezanpour, M. Maerefat, N. Ramezanpour, M. Mokhtari-Dizaji, F. Roshanali, and . Rikhtegar Nezami. Numerical investigation of the effects of bed shape on the end-to-side cabg hemodynamics. *Journal of Mechanics in Medicine and Biology*, 19(4):1950019, 2019. doi: 10.1142/s0219519419500192.

G. Santesarti, M. Marino, F. Viola, R. Verzicco, and G. Vairo. An insight into parameter identifiability issues in the Carreau-Yasuda model: A more consistent rheological formulation for shear-thinning non-newtonian inelastic fluids. *Journal of Non-Newtonian Fluid Mechanics*, page 105438, 2025. doi: 10.1016/j.jnnfm.2025.105438.

A. Sarraju and S. E. Nissen. Atherosclerotic plaque stabilization and regression: a review of clinical evidence. *Nature Reviews Cardiology*, 21(7):487–497, 2024. doi: 10.1038/s41569-023-00979-8.

J.h M. Sherwood, E. Kaliviotis, J. Dusting, and S. Balabani. Hematocrit, viscosity and velocity distributions of aggregating and non-aggregating blood in a bifurcating microchannel. *Biomechanics and Modeling in Mechanobiology*, 13(2):259–273, 2014. doi: 10.1007/s10237-012-0449-9.

G. B. Thurston. Rheological parameters for the viscosity viscoelasticity and thixotropy of blood. *Biorheology*, 16:149–162, 1979. doi: 10.3233/BIR-1979-16303.

A. G. Van der Giessen, H. C. Groen, P.A. Doriot, P. J. De Feyter, A. FW. Van der Steen, F. N. Van de Vosse, J. J. Wentzel, and F. JH. Gijsen. The influence of boundary conditions on wall shear stress distribution in patients specific coronary trees. *Journal of Biomechanics*, 44(6):1089–1095, 2011. doi: 10.1016/j.jbiomech.2011.01.036.

C. Zhang, S. Xie, S. Li, F. Pu, X. Deng, Y. Fan, and D. Li. Flow patterns and wall shear stress distribution in human internal carotid arteries: the geometric effect on the risk for stenoses. *Journal of Biomechanics*, 45(1):83–9, 2012. doi: 10.1016/j.jbiomech.2011.10.001.